

# Bose-Einstein correlations from opaque sources

Henning Heiselberg<sup>1</sup>, Axel P. Vischer<sup>2</sup>

<sup>1</sup> NORDITA, Blegdamsvej 17, DK-2100 Copenhagen Ø., Denmark

<sup>2</sup> Niels Bohr Institute, DK-2100, Copenhagen Ø, Denmark

Received: 20 March 1997

**Abstract.** Bose-Einstein correlations in relativistic heavy ion collisions are very different for opaque sources than for transparent ones. The Bose-Einstein radius parameters measured in two-particle correlation functions depend sensitively on the mean free path of the particles. In particular we find that the outward radius parameter for an opaque source is *smaller* than the sideward radius parameter for sufficiently short duration of emission. A long duration of emission can compensate the opacity reduction of the longitudinal radius parameter and explain the experimental measurements of very similar side- and outward radius parameters.

## 1 Introduction

Bose-Einstein interference of identical particles (pions, kaons, etc.), emitted from the collision zone in relativistic heavy ion collisions shows up in correlation functions and is an important tool for determining the source at freeze-out. It is commonly assumed that the source is cylindrical symmetric around the beam axis and *transparent*, meaning that the detector receives particles from all over the source. The radius parameter outwards or towards the detector,  $R_o$ , is found to be *larger* [1,2] than the radius parameter,  $R_s$ , sideways or perpendicular to the detector

$$R_o^2 = R_s^2 + \beta_o^2 \delta\tau^2, \quad (1)$$

for particles of zero rapidity. The excess is due to the duration of emission,  $\delta\tau$ , of the source in which particles with transverse momentum  $p_\perp$  and outward velocity  $\beta_o = p_\perp/m_\perp$  travel a distance  $\beta_o \delta\tau$  towards the detector. Distances perpendicular to this velocity like, for example,  $R_s$  are not affected by the duration of emission and thus reflect the “true” transverse size of the source, i.e., the region over which the source can be considered homogeneous. When flow is included the relation (1) is still valid in the analyses of [1,2] whereas strong flow coupled to surface emission can reduce  $R_o$  more than  $R_s$  [3] as well as an ellipsoidal source [4,5].

Experimentally the HBT radius parameters,  $R_{s,o,l,ol}$ , are extracted from measurements of the two-pion and two-kaon correlation function by parametrizing it with the common gaussian form

$$C(q_s, q_o, q_l) = 1 + \lambda \exp(-q_s^2 R_s^2 - q_o^2 R_o^2 - q_l^2 R_l^2 - 2q_o q_l R_{ol}^2). \quad (2)$$

Surprisingly, in relativistic heavy ion collisions the outward and sideward radius parameters are measured to be

similar [6–10] (and in a few cases the outward size is even measured to be smaller than the sideward size [6,7] contradicting (1)) within experimental uncertainty. According to (1) this implies that particles freeze-out suddenly,  $\delta\tau \ll R_i$ , as in a “flash” [11], in particular when resonance life-times are included [4,12].

We want to point out that an *opaque* source emitting *away* from its surface naturally leads to  $R_o \ll R_s$  unless the duration of emission,  $\delta\tau$ , is very long. There is therefore a strong correlation between the direction of the emitted particles and the emission zone - contrary to cylindrically symmetric transparent sources without flow. In our model the measured sideward radius parameter samples the full source size, while the measured outward radius parameter sample only a small surface region of the opaque source in the direction of the emitted particles. The opaque source is inspired by hydrodynamical as well as cascade calculations of particle emission in relativistic heavy ion collisions. In hydrodynamical calculations particles freeze-out at a hypersurface that generally does not move very much transversally until the very end of the freeze-out [13]. However, most hydrodynamical freeze-out mechanisms as well as the analysis in [3] do not include the directional condition that particles can only be emitted away from the surface, though strong flow at the surface has a similar effect. In cascade codes the last interaction points are also found to be distributed in transverse direction around a mean value that does not change much with time [14–16]. The thickness of the emission layer is related to the particle mean free path  $\lambda_{mfp}$ , and is zero in hydrodynamical calculations but several  $fm$ 's in cascade codes. We shall in Sect. 2 consider the parameters  $R$  and  $\lambda_{mfp}$  as constants and in Sect. 3 discuss effects of moving surfaces, temporally dependent emission layers and transverse flow.

## II Surface emission and HBT radius parameters

To quantify our statements we calculate the radius parameters  $R_{s,o,l}$  for two simple sources commonly employed to describe relativistic and ultrarelativistic heavy ion collisions, namely a spherical and a cylindrical symmetric but longitudinally expanding source. However, we add the important requirement that the source should be opaque emitting away from a surface layer of thickness  $\sim \lambda_{mfp}$ .

For the correlation function analysis of Bose-Einstein interference from a source of size  $R$  we consider two particles emitted a distance  $\sim R$  apart with relative momentum  $\mathbf{q} = (\mathbf{k}_1 - \mathbf{k}_2)$  and average momentum,  $\mathbf{K} = (\mathbf{k}_1 + \mathbf{k}_2)/2$ . Typical heavy ion sources in nuclear collisions are of size  $R \sim 5$  fm, so that interference occurs predominantly when  $q \sim \hbar/R \sim 40$  MeV/c. Since typical particle momenta are  $k_i \simeq K \sim 300$  MeV, the particles escape almost parallel (see Fig. 1), i.e.,  $k_1 \simeq k_2 \simeq K \gg q$ . The correlation function due to Bose-Einstein interference of identical particles from an incoherent source is (see, e.g., [1])

$$C(\mathbf{q}, \mathbf{K}) = 1 + \left| \frac{\int d^4x S(x, \mathbf{K}) e^{iqx}}{\int d^4x S(x, \mathbf{K})} \right|^2, \quad (3)$$

where  $S(x, \mathbf{K})$  is a function describing the phase space density of the emitting source. With  $qx = \mathbf{q} \cdot \mathbf{x} - \mathbf{q} \cdot \boldsymbol{\beta}_K t$ , where  $\boldsymbol{\beta}_K = \mathbf{K}/E_K$  is the pair velocity, one can, by expanding to second order in  $q_i R_i$  and compare to (2), find the radius parameters  $R_i$ ,  $i=s,o,l,ol$ , [1]

$$R_i^2 = \sigma(x_i - \beta_i t), \quad R_{ol}^2 = \langle (x_o - \beta_o t)(x_l - \beta_l t) \rangle, \quad (4)$$

where the source average of a quantity  $\mathcal{O}$  and its fluctuation are defined by

$$\langle \mathcal{O} \rangle \equiv \frac{\int d^4x S(x, K) \mathcal{O}}{\int d^4x S(x, K)}, \quad \sigma(\mathcal{O}) \equiv \langle \mathcal{O}^2 \rangle - \langle \mathcal{O} \rangle^2. \quad (5)$$

The reduction factor  $\lambda$  in (2) may be due to long lived resonances [12, 4], coherence effects, incorrect Gamov corrections [17] or other effects. It is found to be  $\lambda \sim 0.5$  for pions and  $\lambda \sim 0.9$  for kaons.

Generally a particle is emitted and escapes after it has made its final interaction with any of the other particles in the source. If the source is dense it is more probable to emit from the surface than from the center. In Glauber theory particles are emitted from a surface layer with a depth of order of the mean free path,  $\lambda_{mfp}$ , with probability

$$S(x, \mathbf{K}) \sim \exp\left(-\int_x^\infty dx' \sigma n(x')\right) = \exp(-l/\lambda_{mfp}). \quad (6)$$

Here the integral runs over the particle trajectory from emission point  $x$  to the detector. Assuming an average density  $n$  in the emission layer, the distance  $l$ , that the particle has to pass through is of order of the mean free path,  $\lambda_{mfp} = 1/\sigma n$  (see Fig. 1). A similar surface layer was introduced by Grassi et al. [18] in order to improve

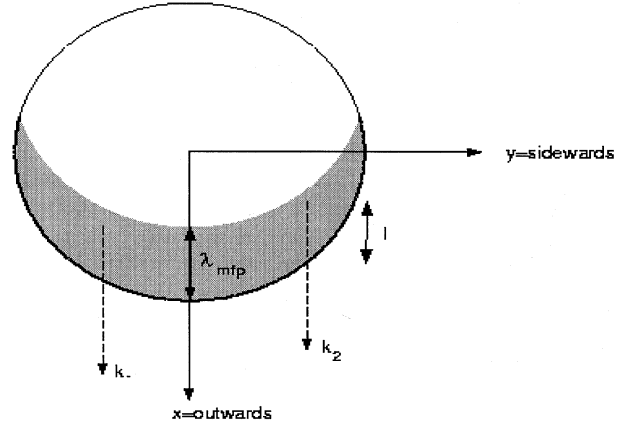


**Fig. 1.** Cross section of the interaction region perpendicular to the longitudinal or  $z$ -direction. Particles have to penetrate a distance  $l$  out to the surface of the interaction region in order to escape and reach the detector. The bulk part of the emitted particles comes from a surface region of width  $\lambda_{mfp}$ , the mean free path of the particle

the standard Cooper-Frye freeze-out in hydrodynamical calculations and to study the effect on transverse momentum spectra.

In the following subsection we assume that the source size  $R$  and thickness of emission layer  $\lambda_{mfp}$  are constants in time. In Sect. 3 we will generalize these results including temporal dependences in connection with the final freeze-out of the source.

### A Spherical sources

First we investigate a spherically symmetric source of radius  $R$ . Including the temporal evolution of the source emission function by  $S_t(t)$ , the phase space density of the source will have the approximate form

$$S(x, K) \sim \Theta(R^2 - x^2 - y^2 - z^2) e^{-l/\lambda_{mfp}} S_t(t). \quad (7)$$

For strict surface emission<sup>1</sup> ( $\lambda_{mfp} = 0$ ) the source reduces to

$$S(x, K) \sim \cos \theta \Theta(\cos \theta) \delta(R^2 - x^2 - y^2 - z^2) S_t(t). \quad (8)$$

where  $\theta$  is the polar angle with respect to the outward direction along  $\mathbf{K}$ ; we will in the following orient our cartesian axes such that the  $x$ -axis is in the outward direction. The geometric factor  $\cos \theta = x/R$  suppresses the peripheral zones and the  $\Theta(\cos \theta) = \Theta(x)$  factor insures that particles are only emitted *away* from the surface, i.e., only particles from the surface layer of the half hemisphere directed towards the detector will reach it whereas particles

<sup>1</sup> A spherical source similar to (8) with strict surface emission,  $\lambda_{mfp} = 0$ , was applied to proton emission from excited nuclei [19]. As proton decay times are long only the finite duration of emission contribution was considered (i.e, the last term in (9).)

from the other hemisphere will interact on their passage through the source.

The temporal emission is determined by  $S_t(t)$ . It is commonly approximated by a gaussian,  $S_t(t) \sim \exp(-(t-t_0)^2/2\delta t^2)$ , around the source mean life-time,  $\tau_0$  with width or fluctuation,  $\delta\tau$ , which is the duration of emission. These gaussian parameters approximate the average emission time,  $\langle t \rangle$  and the variance or fluctuation,  $\sigma(t)$ , for a general source, respectively.

Orienting our coordinate system with outward or x-axis along  $\mathbf{K}$  we have  $\beta_{\mathbf{K}} = \mathbf{K}/E_{\mathbf{K}} = (\beta_o, 0, 0)$  (see Fig. 1) when the pair rapidity has been boosted longitudinally to their center-of-mass system,  $Y = 0$ . In that case  $l = (\sqrt{R^2 - y^2 - z^2} - x)$ . When  $\lambda_{mfp} \ll R$  we obtain from equations (3-5)

$$R_o^2 = \frac{1}{18}R^2 + \frac{29}{36}\lambda_{mfp}^2 + \beta_o^2\sigma(t), \quad (9)$$

$$R_s^2 = \frac{1}{4}R^2 - \frac{1}{8}\lambda_{mfp}^2, \quad (10)$$

$$R_l^2 = R_s^2, \quad (11)$$

and  $R_{ol}$  vanishes. Aside from the  $\beta_o^2 \sigma(t)$  term, we notice that an opaque ( $\lambda_{mfp} \ll R$ ) source has  $R_o^2 = 2R_s^2/9$ , i.e., the outward radius parameter seems much smaller than the actual source size as well as  $R_s$ . This is a simple geometrical effect that arises because no particles are observed from the dark side of the source (see Fig. 1) leading to an expectation value of  $\langle x \rangle$  that is displaced from the center and only slightly smaller than  $\sqrt{\langle x^2 \rangle}$ . For comparison, a transparent ( $\lambda_{mfp} = \infty$ ) and spherically symmetric source has the same extent in all directions and one finds  $R_s = R_o = R_l = R/\sqrt{5}$ . Including the term due to the duration of emission,  $\beta_o^2 \sigma(t)$ , the outward HBT radius parameter is necessarily larger than the sideward.

## B Cylindrical sources

At very high energies longitudinal expansion is important and we employ a locally thermal but longitudinally expanding (with Bjorken flow  $u = z/t$ ) source as in [1,2]

$$S(x, K) \sim \Theta(R^2 - x^2 - y^2) \times \exp\left(-\frac{m_{\perp} \cosh(Y - \eta)}{T} - \frac{l}{\lambda_{mfp}}\right) S_{\tau}(\tau). \quad (12)$$

Here,  $\tau = \sqrt{t^2 - z^2}$  is the invariant or proper time and  $\eta = 0.5 \ln(t+z)/(t-z)$  the space-time rapidity.  $R$  is the transverse source size,  $m_{\perp}$  the transverse mass and  $Y$  the rapidity of the particles. The distance that the particles have to pass through matter in the transverse direction is  $l \simeq (\sqrt{R^2 - y^2} - x)$ . Actually, when  $\eta \neq Y$  the particles pass a distance longitudinally, which will lead to a minor reduction of  $R_l$ , but as we concentrate on the transverse radius parameters we will ignore this effect in the following. From equations (3-5) we obtain when  $\lambda_{mfp} \ll R$

$$R_o^2 = \left(\frac{2}{3} - \left(\frac{\pi}{4}\right)^2\right)R^2 + \left(\frac{7}{6} - \frac{\pi^2}{32}\right)\lambda_{mfp}^2$$

$$+ \beta_o^2 \sigma(\tau), \quad (13)$$

$$R_s^2 = \frac{1}{3}R^2 - \frac{1}{6}\lambda_{mfp}^2, \quad (14)$$

$$R_l^2 \simeq \langle \tau^2 \rangle \frac{T}{m_{\perp}}, \quad (15)$$

for  $Y = 0$  (which leads to  $R_{ol} = 0$ ) and keeping only leading orders in  $\sigma(\tau)$  and  $T/m_{\perp}$  (see, e.g., [1] for higher orders). Again we notice that for a short-lived ( $\beta_o \sigma(\tau)^{1/2} \ll R$ ) and opaque ( $\lambda_{mfp} \ll R$ ) source the outward radius parameter seems much smaller than the actual source size as well as the sideward radius parameter,  $R_o = 0.22R = 0.39R_s$  (see Fig. 2). For a short-lived transparent source ( $\lambda_{mfp} = \infty$ ) the transverse radius parameters are the same  $R_s = R_o = R/2$ . The experimental measurements find, that  $R_o \sim R_s$ . This implies a very long duration of emission,  $\beta_o \sigma(\tau)^{1/2} \sim R_s$ , for an opaque source and is in sharp contrast to the very short duration of emission the same data would imply for a transparent source.

## III Temporal dependence and freeze-out

Eventually all particles created in the high energy nuclear collisions must freeze-out. In cascade codes the emission changes from strict surface emission shortly after the collision starts to an emission layer, which increases in thickness to the size of the system. At this stage volume emission takes over and, aside from long lived resonance decays, the source freezes out [14–16]. This picture is somewhat different in hydrodynamic codes, where the emission is strictly from the surface at all times, but the surface eventually moves inward and the source freeze out when the surface hits the center [13]. However, just before freeze-out the hydrodynamic hypersurface moves inward with superluminal speed. Again this stage is better characterized by volume freeze-out rather than by surface emission. The hydrodynamic results may become more similar to those of the cascade models, if we include emission from a surface layer of finite thickness, as in [18], as well as a cascade among the hadronized particles.

The freeze-out can be described by allowing the layer of emission or  $\lambda_{mfp}$  to increase with time after the collision. According to the Bjorken scaling model the mean free path increases linearly with proper time  $\tau$

$$\lambda_{mfp}(\tau) = \frac{1}{\bar{\sigma}n(\tau)} = \frac{\pi R^2}{\bar{\sigma}dN/dy} \tau \equiv \lambda_{mfp}(\tau_f) \frac{\tau}{\tau_f}, \quad (16)$$

since the particle density drops inversely with proper time due to the one-dimensional expansion in longitudinal direction. In cascade codes the size of the emission layer also increases with time up to freeze-out. Assuming such a linear increase a simple estimate of the HBT radius parameters can be made. From the definition in (4) we find, that the HBT radius parameters are the time-averaged values of the  $\lambda_{mfp}$  dependent HBT radius parameters

$$R_i^2 = \frac{2}{\tau_f^2} \int_0^{\tau_f} R_i^2(\lambda_{mfp}(\tau)) \tau d\tau$$

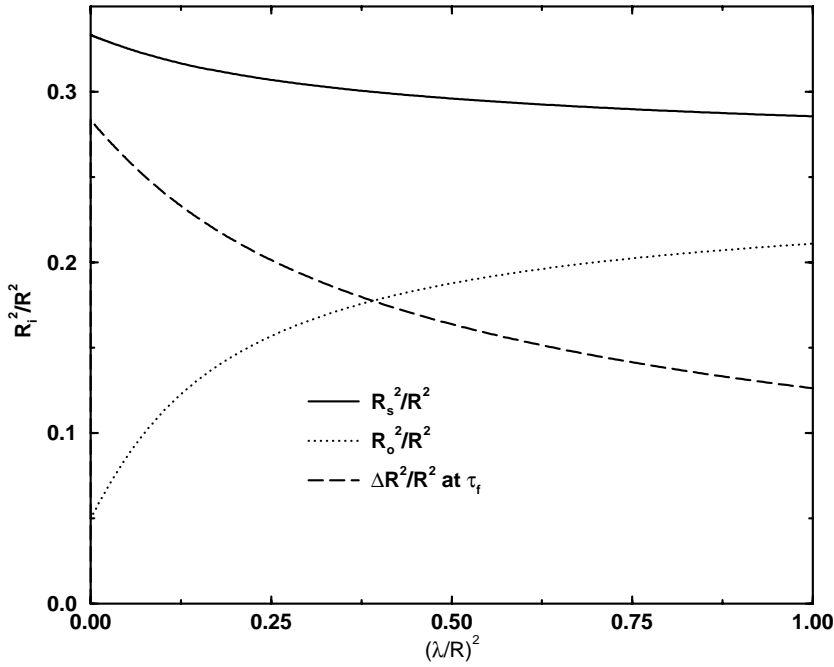


**Fig. 2.** Sideward and outward HBT radius parameters as function of the relative thickness of surface layer thickness to source size. The small mean free path limits are given in equations (9) and (10) and for  $\lambda_{mfp} \gg R$  they approach  $R_s = R_o = R/2$ . The duration of emission contribution  $\beta_o^2 \sigma(\tau)$  is not included in  $R_o^2$ . The strength of the opacity effect,  $\Delta R^2/R^2$ , is estimated from (18) at the freeze-out time  $\tau_f$

$$= \int_0^{\lambda_{mfp}^2(\tau_f)} R_i^2(\lambda_{mfp}(\tau)) \frac{d\lambda_{mfp}^2}{\lambda_{mfp}^2(\tau_f)}. \quad (17)$$

Thus the HBT radius parameters are the average values of the mean free path dependent radius parameters of Fig. 2 up to  $\lambda_{mfp}^2(\tau_f)$ . If we include now the duration of emission the difference is

$$\begin{aligned} R_o^2 - R_s^2 &= \int_0^{\lambda_{mfp}^2(\tau_f)} \\ &\times (R_o^2(\lambda_{mfp}) - R_s^2(\lambda_{mfp})) \frac{d\lambda_{mfp}^2}{\lambda_{mfp}^2(\tau_f)} + \beta_o^2 \sigma(\tau) \\ &\equiv -\Delta R^2 + \beta_o^2 \sigma(\tau). \end{aligned} \quad (18)$$

Here  $\Delta R^2$  is the average distance between  $R_s^2$  and  $R_o^2$  in Fig. 2, i.e., the area between the curves for  $R_s^2$  and  $R_o^2$  up to  $\lambda_{mfp}^2(\tau_f)$  and divided by that same factor  $\lambda_{mfp}^2(\tau_f)$ . The opacity difference  $\Delta R^2$  is plotted as dashed line in Fig. 2. Though it decreases with increasing  $\lambda_{mfp}(\tau_f)$ , it is a substantial fraction of  $R_s^2$  for mean free paths at freeze-out of order the size of the system.

It is instructive to consider the recent and relevant example of central  $Pb+Pb$  collisions at energy 160 A·GeV. The NA44 data finds for the pion HBT radius parameters  $R_s \simeq R_o \sim 4.5 - 5.0$  fm and  $R_l \simeq 5 - 6$  fm [6]. The average transverse momentum was  $p_\perp \simeq 165$  MeV such that  $\beta_o = p_\perp/m_\perp \simeq 0.76$ . From the transverse momentum slopes of pions, kaon, protons and deuterium in [20] one finds a temperature  $T \sim 120$  MeV and transverse flow  $v \sim 0.6c$ . Larger transverse flow and smaller temperatures can, however, not be excluded. The transverse flow effect on the HBT radius parameters is small for these  $p_\perp$  and  $v$  values [21]. If we assume that the source emits pions at a constant rate per surface element, we can estimate from

the longitudinal HBT radius parameter, (15), the freeze-out time  $\tau_f = (2 m_\perp/T)^{1/2} R_l \sim 11$  fm/c. As seen from equations (14) the sideward radius parameter is relatively less affected by the  $\lambda_{mfp}^2$  term and we extract an initial transverse source size  $R \sim 3^{1/2} R_s \sim 9$  fm from the NA44 sideward HBT radius parameter.

To determine the outward HBT radius parameter we have to estimate the mean free path, for example, from (16). In central  $Pb + Pb$  collisions at 160 A·GeV the particle rapidity density is  $dN/dy \sim 600$  around midrapidity. If we take for the pion cross section  $\bar{\sigma}_\pi \sim 20$  mb, the resulting mean free path is very small,  $\lambda_{mfp}(\tau_f) \sim 1$  fm. However, near the surface the density will be lower than the average density used in this estimate and we would rather expect  $\lambda_{mfp}(\tau_f) \sim R$  since pion freeze-out occur when their mean free path is of order the size of the system. For example,  $\Delta R^2 \simeq 0.13$  (0.07)  $R^2$  for  $\lambda_{mfp} = 1.0$  (2.0)  $R$  respectively and the opacity effect leads to a corresponding difference  $\Delta R^2 \simeq 16$  (9) fm<sup>2</sup>. Equation (18) clearly demonstrates the significance of the opacity effect in reducing the outward radius parameter with respect to the sideward. The duration of emission compensates this difference to some extent. Assuming constant particle emission per surface element up to freeze-out, we find  $\beta_o^2 \sigma(\tau) = \beta_o^2 \tau_f^2/18 \simeq 4$  fm<sup>2</sup>. This contribution due to the duration of emission is thus smaller than the reduction due to the opacity contribution and consequently one would expect  $R_o < R_s$ . However, a number of other fluctuations such as moving surfaces, short lived resonances, and other effects also add to  $R_o^2$  [21].

We notice that the transverse source size is only a few  $fm$  larger than the geometrical size of lead  $Pb \sim 7$  fm. Some small expansion of the source seems to take place before final freeze-out. The average emission time is  $\sqrt{\langle \tau^2 \rangle} = \tau_f/\sqrt{2} \simeq 8$  fm/c. This result is entirely consis-

tent with the freeze-out time needed to explain the enhancement in the  $\pi^-/\pi^+$  ratio at low  $p_\perp$  in the same  $Pb + Pb$  collisions due to Coulomb repulsion [22].

## IV Summary and outlook

We have addressed the significant difference in HBT radius parameters between opaque and transparent sources and have calculated the radius parameters and their dependence on the mean free path for simple spherical and longitudinal expanding models. A short-lived and very opaque source or “black body” has much smaller outward than sideward radius parameter. However, a long duration of emission as well as other fluctuations can compensate the reduction due to the opacity effect leading to comparable  $R_o \simeq R_s$  as measured in several experiments. In the case of central  $Pb+Pb$  collisions at 160 A·GeV the opacity reduction was estimated to be a significant fraction of the outward HBT radius parameter and larger than the contribution from a source emitting during all its life-time. Other fluctuations like moving surfaces, short lived resonances, and other effects do, however, also add to  $R_o^2$  and we expect that this is the reason that the sideward and outward HBT radius parameters are measured to be very similar in relativistic heavy ion collisions. We find that pions do not appear as in a “flash”. In fact a long duration of emission of order the life-time of the source is possible and consistent with an outward HBT radius parameter smaller or comparable to the sideward due to the opacity effect. In contrast, a simple transparent source would necessarily have a very short duration of emission as implied by (1).

The Cooper-Frye freeze-out condition in hydrodynamic models does not take the opacity effect into account and generally one finds considerably larger outward than sideward source radius parameters due to the long freeze-out time [13]. Cascade codes have implicitly opacities build in through rescatterings and do find a directional effect [14], but also long duration of emission and mean free paths [15] are found leading to larger outward radius parameters than sideward.

Other effects like, e.g., transverse flow, can also reduce the outward HBT radius parameter more than the sideward. At larger transverse momenta the sideward and outward HBT radius parameters are reduced by transverse flow and the longitudinal scales by the factor  $1/m_\perp$ . This may explain the decrease of all the HBT radius parameters with increasing  $p_\perp$  as found in the NA44 experiments [6].

By studying the rapidity and  $p_\perp$  dependence of the HBT radius parameters the duration of emission contribution,  $\beta_o^2 \sigma(\tau)$ , may be separated from the opacity effect,  $\Delta R^2$ , as well as other fluctuations. However, this may be non-trivial if the mean free path, duration of emission and resonance contributions are rapidity and  $p_\perp$  dependent. Transverse flow may also add a strong  $p_\perp$  dependence of the radius parameters but the magnitude of transverse flow can approximately be determined from transverse momentum spectra [20]. HBT radius parameters and

transverse flow increase for heavier ions colliding. The nuclear  $A$ -dependence can therefore provide additional information on freeze-out times, sizes, transverse flow and opacity of the sources.

*Acknowledgements.* We would like to thank Larry McLerran and Scott Pratt for stimulating discussions.

## References

1. S. Chapman, J.R. Nix, and U. Heinz, Phys. Rev. **C52**, 2694 (1995); S. Chapman, U. Heinz and P. Scotto, Heavy Ion Physics **1,1** (1995); U. Heinz, Nucl. Phys. **A610** (1996) 264c
2. T. Csörgő, Phys. Lett. **B347**, 354 (1995); T. Csörgő and B. Lörstad, Nucl. Phys. **A590**, 465c (1995); and Phys. Rev. **C54** (1996) 1390
3. S. Pratt, Phys. Rev. Lett. **53** (1984) 1219
4. T. Csörgő and B. Lörstad, Z. Physik **C71**, 491 (1996)
5. W. E. Cleveland and S. A. Voloshin, Phys. Rev. **C** 1996, in press
6. H. Beker et al. (NA44 collaboration), Phys. Rev. Lett. **74** (1995) 3340; Phys. Lett. **B 302** (1993) 510; H. Bøggild et al., Phys. Lett. **B 349** (1995) 386
7. A. Franz, (NA44 collaboration), Nucl. Phys. A **610** (1996) 240c
8. T. Alber et al. (NA35 and NA49 collaborations), Nucl. Phys. **A 590** (1995) 453c; Z. Physik. **C 66** (1995) 77; K. Kadija et al. (NA49 collaboration), Nucl. Phys. A **610** (1996) 248c; D. Ferenc et al., Nucl. Phys. **A 544** (1992) 531c
9. T.C. Awes et al. (WA80 collaboration), Z. Physik. **C 65** (1995) 207; *ibid.* **C 69** (1995) 67. T. Abbott et al. (E802 collaboration), Phys. Rev. Lett. **69** (1992) 1030
10. J. Barrette et al. (E877 collaboration), Nucl. Phys. **A 590** (1995) 259c
11. T. Csörgő and L.P. Csernai, Phys. Lett. **B333**, 494 (1994)
12. H. Heiselberg, Phys. Lett. **B379**, 27 (1996)
13. J. Bolz, U. Ornik, M. Plümer, B.R. Schlei, and R.M. Weiner, Phys. Rev. **D 47** (1993) 3860; J. Sollfrank et al., hep-ph/9607029
14. T. J. Humanic, Phys. Rev. **C 53** (1996) 901
15. J. P. Sullivan, M. Berenguer, B.V. Jacak, M. Sarabura, J. Simon-Gillo, H. Sorge, H. van Hecke, S. Pratt, Phys. Rev. Lett. **70** (1993) 3000
16. L. V. Bravina, I. N. Mishustin, N. S. Amelin, J. P. Bondorf, L. P. Csernai, Phys. Lett B **354** (1995) 196
17. G. Baym and P. Braun-Munzinger, Nucl. Phys. A **610** (1996) 286c
18. F. Grassi, Y. Hama and T. Kodama, Phys. Lett. **B 355** (1995) 9
19. G.I. Kopylov and M.I. Podgoretskii, Sov. J. Nucl. Phys. **15** (1972) 219; *ibid.* **18** (1974) 336
20. I. G. Bearden et al. (NA44 collaboration), Phys. Rev. Lett. **78** (1997) 2080
21. H. Heiselberg and A.P. Vischer, to be published, nucl-th/9703030
22. H.W. Barz et al., Proc. of Hirschegg meeting, Jan. 13–17, 1997